Published in final edited form as:
Acta Biomater. 2012 April ; 8(4): 1430–1439. doi:10.1016/j.actbio.2011.12.031.

Incorporation of phosphate group modulates bone cell attachment and differentiation on oligo(polyethylene glycol) fumarate hydrogel

Mahrokh Dadsetan[a], **Melissa Giuliani**[a,c], **Florian Wanivenhaus**[a,d], **M. Brett Runge**[a], **Jon E. Charlesworth**[b], and **Michael J. Yaszemski**[a,*]

[a]Department of Orthopedic Surgery, Mayo Clinic College of Medicine, 200 First Street SW, Rochester, MN 55905, USA

[b]Department of Biochemistry and Molecular Biology, Mayo Clinic College of Medicine, 200 First Street SW, Rochester, MN 55905, USA

[c]Antioquia School of Engineering, Medellin, Colombia

[d]Paracelsus Medical University, Strubergasse 21, 5020 Salzburg, Austria

Abstract

In this work, we have investigated the development of a synthetic hydrogel that contains a negatively charged phosphate group for use as a substrate for bone cell attachment and differentiation in culture. The photoreactive, phosphate-containing molecule, bis(2-(methacryloyloxy)ethyl)phosphate (BP), was incorporated into oligo(polyethylene glycol) fumarate hydrogel and the mechanical, rheological and thermal properties of the resulting hydrogels were characterized. Our results showed changes in hydrogel compression and storage moduli with incorporation of BP. The modification also resulted in decreased crystallinity as recorded by differential scanning calorimetry. Our data revealed that incorporation of BP improved attachment and differentiation of human fetal osteoblast (hFOB) cells in a dose-dependent manner. A change in surface chemistry and mineralization of the phosphate-containing surfaces verified by scanning electron microscopy and energy dispersive X-ray analysis was found to be important for hFOB cell attachment and differentiation. We also demonstrated that phosphate-containing hydrogels support attachment and differentiation of primary bone marrow stromal cells. These findings suggest that BP-modified hydrogels are capable of sustaining attachment and differentiation of both bone marrow stromal cells and osteoblasts that are critical for bone regeneration.

Keywords

Hydrogel; Bone regeneration; Osteoblast; Rabbit marrow stromal cells

*Corresponding author. Tel.: +1 507 284 3747; fax: +1 507 284 5075. yaszemski.michael@mayo.edu (M.J. Yaszemski).

Conflicts of Interest

A non-provisional patent has been filed for photocrosslinkable oligo(polyethylene glycol) fumarate used in this research, and this technology has been licensed to BonWrx.

1. Introduction

Creation of a functional polymer surface that mimics the bone extracellular matrix is necessary to direct biomineralization and stimulate cell adhesion, migration and proliferation [1,2]. Hydroxyapatite- and phosphate-containing coatings have been studied extensively to better integrate biomaterial implants with bone for applications such as hip replacement, dental implants and screws for fracture fixation [3,4]. These coatings provide a bone-like mineral matrix that stimulates the in vivo bone environment. More specifically, a bone-like mineral has been shown to be prerequisite to the attachment of osteoblasts and bonding of orthopedic implant materials to bone tissue (osteoconductivity) and may drive osteogenic differentiation of adult stem cells (osteoinductivity) [5]. Hydroxyapatite coatings adsorb many proteins and other macromolecules and lead to a biological layer that favors cell attachment and osteogenic differentiation [6]. However, there are disadvantages associated with the coating of minerals on the polymer surfaces, including poor adhesion and the lack of a structural relationship between the surface and mineral layer [7,8]. More recent studies have focused on chemically altering the polymer interface [9–11]. These approaches include post-processing of the polymer matrix to initiate mineral nucleation and/or creating mineralization nucleators with covalent linkages within the polymer network.

Polyethylene glycol (PEG)-based hydrogels have been extensively studied for their use in tissue engineering and regenerative medicine applications [12–14]. The drawback of PEG-based hydrogels is a low cell attachment rate as a result of the formation of a hydrated surface layer that inhibits adsorption of adhesion proteins such as fibronectin. Investigators have applied a variety of techniques to improve cell adhesion on PEG-based hydrogels. This includes incorporation of adhesion peptides such as arginine-glycine-aspartic acid (RGD)-peptide [15–18] and electrical charge [19–21]. Oligo(polyethylene glycol) fumarate (OPF) is an injectable and biodegradable PEG-based hydrogel previously used in our group for cartilage tissue engineering and nerve regeneration [19,22]. We have reported that the physical and chemical properties of OPF hydrogels can be modified by incorporation of a positively charged monomer [2-(methacryloyloxy) ethyl]-trimethylammonium chloride (MAETAC), and positively charged OPF promoted neurite outgrowth from primary neuronal cells [19].

In this study, we have hypothesized that incorporation of phosphate groups into OPF scaffolds facilitates mineral nucleation and improves osteogenesis. To test our hypothesis, bis(2-(methacryloyloxy) ethyl) phosphate (BP) which consists of two photoreactive methacrylate groups and a pendant phosphate group has been incorporated into the OPF hydrogel. The effects of BP on hydrogel swelling, rheological, mechanical and thermal properties have been investigated. Additionally, we have evaluated the effects of the phosphate group on attachment and differentiation of both immortalized human fetal osteoblast (hFOB) cell line and primary rabbit marrow stromal cells.

2. Materials and methods

2.1. Synthesis

OPF was synthesized using PEG with an M_n of 10,000, according to a previously described method [18]. Briefly, 50 g dried PEG was placed in an ice bath and purged with nitrogen for 10 min. Then, 0.9 mol triethylamine (TEA; Aldrich, Milwaukee, WI) per mol PEG and 1.8 mol distilled fumaryl chloride (Acros, Pittsburgh, PA) per mol PEG were added dropwise, and stirred at room temperature for 48 h. For purification, methylene chloride was removed, and OPF was crystallized in ethyl acetate.

2.2. Hydrogel fabrication

OPF hydrogels were fabricated as previously described with addition of photoinitiator (Irgacure 2959, donated by Ciba-Specialty Chemicals) and *N*-vinyl pyrrolidinone (NVP; Aldrich, Milwaukee, WI) [23]. Bis(2-(methacryloyloxy)ethyl) phosphate (BP, Aldrich, Milwaukee, WI) was incorporated into OPF at various concentrations (Table 1). To prepare hydrogel films, the hydrogel mixture was pipetted between two glass slides with a 1 mm spacer and polymerized by exposure to UV light for 30 min. Hydrogel discs were vacuum dried after fabrication, weighed (W_i, initial weight) and swollen to equilibrium for 24 h at 37 °C in deionized water. Swollen samples were blotted dry and weighed (W_s, swollen weight), then dried in reduced pressure and weighed again (W_d, final dry weight). The swelling ratio and sol fraction of the hydrogels were calculated using the following equations:

$$\text{Swelling ratio} = (W_s - W_d)/W_d$$
$$\text{Sol fraction} = [(W_i - W_d)/W_I] \times 100$$

2.3. Attenuated total reflectance Fourier transform infrared (ATR-FTIR) spectroscopy

Incorporation of BP into OPF hydrogels was characterized using a micro-ATR-FTIR spectrophotometer (Nicolet 8700), coupled to a Continuum microscope (Thermo Electron Corp., Madison, WI). The microscope used an ATR slide on a germanium crystal and spectra were collected at a resolution of 4 cm^{-1} for 128 scans. The differences in surface composition among the various hydrogel formulations were quantified by measuring the ratios of the characteristic peaks.

2.4. Mechanical and rheological properties

Hydrogel films were cut into discs of 10 mm diameter with a cork borer and swelled in deionized water overnight. Compressive moduli of the swollen hydrogels were determined using a dynamic mechanical analyzer (DMA-2980, TA Instruments, New Castle, DE). Mechanical testing was performed under load control, where load was applied at a rate of 4 N min^{-1}. Stress and strain data collected during testing were plotted, and the storage modulus was determined as the slope of the linear region of the stress vs. strain curve. The linear viscoelastic properties of hydrated cross-linked OPF and OPF-BP polymer films of 8 mm diameter × 1 mm height were measured using a torsional dynamic mechanical analyzer (TA Instruments AR2000 rheometer). An 8 mm parallel plate was used for rheological measurements. A compressive force of 1.5 ± 0.1 N was applied to the hydrogels. The linear viscoelastic region was determined using a strain sweep at a frequency of 1 Hz. A strain of 1.0% was determined to be within the linear viscoelastic region for all polymers and was used for all rheological measurements. A frequency sweep from 0.1 to 628.3 rad s^{-1} was used to measure storage (G') and loss (G'') moduli.

2.5. Thermal characterization

Differential scanning calorimetry (DSC) measurements were performed using a TA Q1000 differential scanning calorimeter in a nitrogen atmosphere. DSC was performed for three consecutive heat/cool/heat cycles. Each sample was preheated from room temperature to 100 °C and cooled to −80 °C at a cooling rate of 5 °C min^{-1}. The last heating cycle was performed from −80 to 150 °C at a heating rate of 5 °C min^{-1}. Thermogravimetric analysis (TGA) was performed on a TA Q500 thermal analyzer at a heating rate of 5 °C min^{-1} from 5 to 800 °C under flowing nitrogen.

2.6. Osteoblast cell culture

The hFOB cell line [24], which contains the temperature-sensitive T-antigen expression vector with the neomycin resistance gene, was maintained at 34 °C in phenol red-free Dulbecco's Modified Eagle's Medium (DMEM)/F12 containing 10% charcoal-stripped fetal bovine serum (FBS; Sigma Chemical Co., St Louis, MO, USA) and supplemented with geneticin (300 $\mu g ml^{-1}$; Gibco/BRL, Rockville, MD, USA). The cells were plated into T-75 flasks at 1×10^6 cells per flask, and maintained in a humidified atmosphere of 5% CO_2 until confluency was achieved, and then trypsinized prior to their use in the experiments.

2.6.1. Toxicity of scaffold leaching materials—hFOB cells were plated on tissue culture at a concentration of 20,000 cells cm^{-2}. After 24 h, transwells containing hydrogels were transferred to the wells with hFOB cells in the culture. After 1 and 3 d exposure to the leaching material from hydrogels, the viability of the cells was tested using the MTS Cell Proliferation Assay (Pro-mega Corporation, Madison, WI), and compared with viability of the cells on tissue culture plates.

2.6.2. Cell viability and attachment—Prior to cell seeding, samples were disinfected with 70% ethanol for 30 min. Ethanol was aspirated and samples were soaked in sterile phosphate-buffered saline (PBS) for 1 h with three changes followed by two changes of media and incubation overnight. An aliquot of 250 μl of the cell suspension containing 15,000 cells were seeded onto the top of the hydrogel discs in 24-well plates fixed with rubber rings and incubated for 2 h to allow the cells to attach. After attachment, 750 μl of media was added to each well, and the medium was changed every 3 d. Cell numbers were determined using an MTS proliferation assay kit as mentioned above. The cell morphology and viability of the seeded cells at days 1, 3 and 7 was examined by using a Live/Dead Kit (Molecular Probes, Eugene, Oregan) as per the kit instructions. This technique stains living cells green and dead cells red. After staining, the cells were visualized using confocal scanning microscopy.

2.6.3. Alkaline phosphatase activity—The alkaline phosphatase (ALP) activity of seeded cells at desired time points was measured according to manufacturer's instruction (Sigma). Briefly, at the end of treatment, the cells were rinsed twice with PBS. Alkaline lysis buffer (0. 3 ml, 0.75 M 2-amino- 2-methyl-1-propanol, pH 10.3) containing *p*-nitrophenol phosphate substrate (2 mg ml^{-1}) was added and the mixture was incubated for 30 min at 37 °C. To stop the reaction, 0.3 ml 50 mM NaOH was added. The samples and standards were diluted in 20 mM NaOH, and the absorbance was measured at 409 nm. ALP activity was normalized to total cellular protein which was determined by the Bradford protein assay (Bio-Rad, Hercules, CA).

2.7. Scanning electron microscopy (SEM) and energy dispersive X-ray analysis (EDAX)

To examine mineral formation on hydrogel surfaces, specimens were swollen in dH_2O and incubated in DMEM/F12 containing 10% FBS without cells at 37 °C for 7 d. After 7 d in media, samples were rinsed briefly in dH_2O, vacuum dried and sputter coated with Au/Pd followed by imaging using a Hitachi S-4700 scanning electron microscope. Samples for EDAX were mounted onto carbon double sticky tape and left uncoated. Specimens were placed in the scanning electron microscope which was operated at 20 kV. Spectra were collected at a magnification of 5000× for 100 s using a Thermo Noran System SIX™ EDS microanalysis system (Middleton, WI). Peak ratios were obtained by measuring the calcium and phosphorus peak heights, and normalizing these to the height of the characteristic carbon peak.

2.8. Mesenchymal stem cell isolation

Using bilateral ileac crest puncture, bone marrow stromal cells were harvested from 2 month old New Zealand White Rabbits. When the cultures were 85% confluent (~14 d), the cells were released from the dish with 0.25% trypsin-EDTA and replated at 250,000 cells per 75 mm plate. MSCs were cultured in low-glucose DMEM supplemented with 10% FBS, and 1% penicillin/streptomycin. The cells used in these studies were at passage 5–6.

2.8.1. MSC culture and characterization—A 250 μl aliquot of the MSC suspension containing 15,000 cells was seeded onto the top of the hydrogel discs in 24-well plates fixed with rubber rings and incubated for 2 h to allow the cells to attach as described above. After attachment 750 μl of media was added to each well, and the medium was changed every 3 d. Cell attachment and viability were characterized as described above. ALP activity of MSCs was measured in both osteogenic and non-osteogenic cell media after 7 d in culture. Osteogenic media was supplemented with 10 nm dexamethasone (Sigma), 2mm β-glycerophosphate (Sigma) and 50 $\mu g ml^{-1}$ L-ascorbic acid phosphate magnesium salt (Wako, Richmond, VA).

2.9. Statistical analysis

The data for hydrogel characterization are reported as means ± standard deviations (SD) for triplicate samples, unless otherwise specified. Single factor analysis of variance (ANOVA) was performed (StatView, version 5.0.1.0, SAS Institute, Inc., Cary, NC) to assess the statistical significance of the results. When the global *F*-test was positive at the 0.05 level, Bonferroni's method was used for multiple comparison tests to determine differences among the experimental groups.

3. Results

3.1. Hydrogel fabrication and characterization

The chemical structures of BP and OPF are shown in Fig. 1. In addition to the phosphate group, BP consists of two methacrylate groups with double bonds which are suitable for crosslinking. BP and OPF are both water soluble and can be mixed at different concentrations and crosslinked in the presence of UV light. As shown in Table 1, five groups of hydrogels were fabricated by varying the ratio of BP concentrations in their formulations. Hydrogels were characterized by measuring their swelling ratio, sol fraction, rheological, mechanical and thermal properties. The swelling ratios of hydrogels significantly increased with addition of BP. The swelling ratios of BP-containing hydrogels were significantly higher than unmodified hydrogel ($P < 0.05$). However, although the swelling ratio of hydrogels remained unchanged with increase in concentration of BP up to 620 μmol, it increased again with the addition of 930 μmol BP to the hydrogel formulation. There was a slight change in the sol fraction of hydrogels when BP was incorporated; however these changes were not statistically significant, except for OPF-BP30, the sol fraction of which was significantly higher than that of unmodified OPF hydrogel (Table 1). The data in Table 1 reveal that the compressive moduli of hydrogels increased from 0.028 to 0.037 MPa with the addition of 310 μmol BP and then decreased as the concentration of BP increased.

Rheology was used to determine the effect that incorporating BP into OPF hydrogels has on the resulting viscoelastic properties. Frequency sweeps were performed to investigate the time-dependent shear behavior, and the storage (G′), loss (G″) moduli and tanδ as a function of angular frequency are shown in Fig. 2. OPF materials exhibit storage and loss moduli independent of low frequencies. High frequencies show that the material stiffens significantly when the shear storage modulus G′ is increased. All materials exhibit cross-

linked properties as G′ > G″ and both values plateau at low frequencies. Incorporation of 5% BP into the OPF hydrogel reduces both G′ and G″ at low frequencies. Higher %BP incorporation does further lower G′ and G″ substantially. OPF-BP materials exhibit a lower tanδ than OPF, indicating they are more elastic than pure OPF.

The thermal properties of unmodified OPF and OPF incorporating BP are compared in Table 2 and Fig. 3. Melting points (Tm), crystallization temperature (Tc) and heats of fusion (ΔTm) were determined from DSC curves. A glass transition temperature (Tg) was not observed in the DSC curves for any of the materials listed in Table 2 (Fig. 3a), because OPF consists of about 98% PEG, which has a strong crystallizability and a high crystallization rate during quenching, resulting in a smaller amorphous fraction and hence difficulty in observing Tg. Table 2 shows that OPF melting point decreased from 57.1 to 53.3 °C upon crosslinking and continued to decrease with incorporation of BP. Unlike Tm, the decrease in heat of fusion (ΔHm) was more robust with both crosslinking and increasing BP concentration. Heat of fusion decreased from 130.9 to 88.9 °C with crosslinking and reached 60 °C when the BP concentration increased to 930 μmol. Likewise, the per cent crystallinity (%C) decreased from 43.2 to 29.1 with increasing BP concentration. As shown in Table 2, the crystallization temperature (Tc) and energy of crystallization (ΔHc) determined in the cooling run decreased with increasing BP concentration, emphasizing the decrease in OPF crystallinity with incorporation of BP. Fig. 3b compares the TGA thermograms of uncrosslinked OPF, OPF and BP-modified OPF. Although TGA was performed on OPF discs after extraction of unreacted materials in water and acetone, there was a weight loss of 1–5% when the hydrogel was heated up to 200 °C. The onset of degradation (Td) for OPF hydrogels varied with incorporation of BP, ranging from 335 to 315 °C. However, thermal degradation of all hydrogels occurred at around 400 °C. BP homopolymer had an onset of degradation of 236 °C which was significantly lower than that for all OPF materials. BP homopolymer lost about 75% of its weight at temperatures up to 700 °C, whereas OPF and BP-modified OPF had a weight loss of 85–99% depending on the BP concentration in the hydrogel formulation. The residue at 700 °C after the degradation of BP-incorporated hydrogels increased proportionally with the composition of BP. The weight fraction of residue for uncrosslinked and crosslinked OPF was 1% and 4%, respectively. The weight fraction of residue for BP-modified materials varied from 5% to 15%, in line with the BP concentration in the hydrogel formulations.

The ATR-FTIR spectra of unmodified, lyophilized OPF hydrogels and OPF hydrogels incorporating BP are compared in Fig. 4a. As shown, after copolymerization of OPF with BP, a new peak emerged at 1725 cm^{-1} that is characteristic of BP methacrylate carbonyl. Unmodified OPF hydrogel has two characteristic peaks at 1085, and 1650 cm^{-1} assigned to PEG C–O bonds and fumarate carbonyl groups, respectively. There is a small peak at 1715 cm^{-1} in the OPF spectrum associated with NVP carbonyl groups. This peak overlaps with the BP carbonyl peak at 1725 cm^{-1}. Comparison of the IR spectra revealed that the peak intensity at 1725 cm^{-1} related to BP increased as the concentration of BP increased, while the peak intensity at 1650 cm^{-1} assigned to OPF decreased on hydrogel surfaces. The relative amount of BP copolymerization in the OPF hydrogels was calculated by comparing the ratios of the OPF absorbance (at its characteristic peak, 1650 cm^{-1}) with the BP absorbance (at its characteristic peak, 1725 cm^{-1}) in the four hydrogel formulations (Fig. 4b). According to this analysis, the amount of BP that actually copolymerized within the OPF hydrogels during the crosslinking process increased linearly (R^2 = 0.9628) as the amount of BP added to the formulation was increased.

3.2. hFOB cell culture

3.2.1. Scaffold toxicity—The toxicity of scaffold leaching materials was tested using hFOB cells. The MTS results reveal that cells remained viable when exposed to the leaching materials from all hydrogel groups and their viability was comparable to our tissue culture plate controls after 1 and 3 d in culture (Fig. 5).

3.2.2. hFOB cell attachment, proliferation and differentiation—Fig. 6 shows greater cell attachment on the surface of OPF-BP10, OPF-BP20 and OPF-BP30 at day 1. By day 3, hFOB cells had round morphology and aggregated on OPF and OPF-BP5 surfaces, while a fibroblast-like morphology was observed for osteoblasts on the scaffolds with higher concentrations of BP. The cells remained viable after 7 d in culture and had higher proliferation rate on OPF-BP10, OPF-BP20 and OPF-BP30. MTS data revealed that initial cell attachment at day 1 did not change on OPF-BP5 as compared to unmodified OPF. However, it increased with increasing BP concentration on OPF-BP10 and thereafter (Fig 7a). At day 3, cell numbers on BP-modified hydrogels were significantly higher than those on unmodified OPF and OPF-BP5. Cell number significantly increased on OPF-BP10, OPF-BP20 and OPF-BP30 hydrogels at days 3 and 7, indicating a significant increase in cell proliferation rate on these hydrogel formulations ($P < 0.05$). ALP activity of hFOB cells on different surfaces are shown in Fig. 7b. ALP activity was similar on unmodified OPF hydrogel, OPF-BP5 and OPF-BP10 at day 1, while it was significantly higher on OPF-BP20 and OPF-BP30 surfaces. By day 7, ALP activity of the hFOB cells cultured on OPF-BP20 and OPF-BP30 was significantly higher than other hydrogel groups.

3.2.3. Mineral nucleation—To assess mineral nucleation on OPF scaffolds, hydrogel samples were incubated in media without cells for 7 d and characterized using SEM and EDAX. The SEM images in Fig. 8a reveal a smooth surface for unmodified OPF while crystal-like particles are seen all over the OPF-BP30 surface. EDAX showed peaks associated with both calcium and phosphorous on the surface of OPF-BP materials. However, there was no peak assigned to calcium and phosphorous on the surface of unmodified OPF. The intensity of phosphorous peaks increased as the concentration of phosphate increased in hydrogel formulations. An increase in calcium peak intensities was also observed with increasing phosphate concentration. However, the Ca/P ratio decreased from 0.6 to 0.2 with increasing phosphate concentration on the hydrogel surfaces (Fig. 8b). Analysis of individual crystals on OPF-BP30 showed a Ca/P ratio of about 0.23, while hydroxyapatite crystals (Berkeley Advanced Biomaterials, Berkeley, CA) had a Ca/P ratio of 1.9.

3.3. MSC culture

3.3.1. MSC attachment—Rabbit MSCs were used to characterize their attachment and differentiation on the surfaces with different compositions. Fig. 9 reveals the attachment, viability and morphology of MSCs on different surfaces at days 1, 3 and 7. MSCs tend to attach more to the BP-incorporating surfaces as compared to unmodified OPF surface. Like osteoblasts, MSCs attached to the surface of BP-incorporating hydrogels in a dose-dependent manner. MTS assay was used for quantification of cell attachment and proliferation (Fig. 10a). The initial cell attachment at day 1 was similar on all hydrogel formulations. However, cell number significantly increased on OPF-BP20 and OPF-BP30 hydrogels after 3 d ($P < 0.05$). At day 7, the number of cells on OPF-BP20 and OPF-BP30 was greater than that of other hydrogel groups and the difference in cell number on these hydrogels was statistically significant as compared to unmodified OPF hydrogel.

3.3.2. ALP activity of MSCs—Fig. 10b compares ALP activity of MSCs on hydrogels of varying compositions in both osteogenic and non-osteogenic media after 7 d in culture. In

non-osteogenic media, the ALP activity of MSCs almost doubled on OPF-BP5 and remained unchanged as the BP concentration increased. Significant differences were found in this media for the ALP activity of the cells cultured on phosphate-containing scaffolds as compared to unmodified surfaces ($P < 0.05$). MSCs exhibited an increased ALP activity in osteogenic media on all surfaces regardless of their composition. However, the differences between ALP activities of the cells on different surfaces were not significant ($P > 0.05$). Additionally, a significant difference was found for ALP activity of the cells cultured on unmodified OPF hydrogel in osteogenic media as compared to non-osteogenic media ($P < 0.05$).

4. Discussion

The initial stage of in vivo biomineralization, such as the nucleation of vertebrate teeth and bone mineralization, occurs through the interaction of immobilized, negatively charged functional groups with calcium and phosphate ions [10]. Although this process is not completely understood, all biomineralization processes are thought to be driven by deposition of an anionic, hydrophilic mineral nucleator on an organic, hydrophobic material, such as collagen in vertebrate skeletons or -chitin in invertebrate exoskeletons [25]. The goal of this study was to develop phosphate-modified hydrogels with properties that could be varied in a controlled manner, and to provide an appropriate substrate for bone cell attachment and differentiation. OPF macromer, copolymerized with varying amounts of negatively charged phosphate-containing monomer (BP), becomes a hydrogel that contains a permanent negative charge for mineral nucleation.

Our data demonstrated that various amounts of BP could be incorporated into the OPF hydrogel, and that swelling ratios of hydrogels increased slightly with incorporation of BP. An increase in compressive modulus of hydrogels was observed with increasing BP concentration up to 310 μmol. However, modulus decreased as BP concentration increased further. These findings correlated well with the sol fraction data where the sol fraction of hydrogels decreased with addition of 310 μmol BP and then increased with increasing BP concentration to 930 μmol. The decrease in the sol fraction is indicative of a highly crosslinked network, and accounts for the increase in the compressive modulus of the BP-modified hydrogels compared to the unmodified hydrogels. However, the use of BP at high concentrations inhibited the OPF crosslinking as indicated by the increased sol fraction. Changes in the viscoelastic behavior of swollen OPF materials were observed with the incorporation of BP. The increase in swelling ratio and the increased sol fraction trend with increasing BP concentrations implies that the lower storage moduli were a result of decreased cross-linking. The increases in lower shear storage modulus was observed for OPF-BP materials compared to OPF; this also correlates with the increased swelling ratio for OPF-BP compositions.

DSC data exhibited a decrease in crystallinity of OPF with both the crosslinking and addition of BP. We demonstrated that incorporation of unsaturated BP monomer increased the frequency of crosslinks between OPF polymer chains as well as OPF chain organization, resulting in a decreased crystallinity. The decrease in crystallinity of PEG hydrogels after crosslinking has been reported by other investigators in our group [26,27]. TGA was performed to determine weight loss when the temperature increases. There was about 5% weight loss when the temperature increased to 200 °C. However, no further weight loss was observed until hydrogels reached their degradation temperature. The weight loss below the temperature of degradation could be due to the loss of either absorbed water or low molecular weight materials. We demonstrated that the onset of degradation temperature (Td) decreased about 30 °C with increasing BP concentration. However, the intermediate value for degradation of all hydrogels was about 400 °C. ATR-FTIR data demonstrated that BP

was successfully incorporated into the OPF hydrogel. FTIR spectra revealed an excellent correlation between the amounts of BP in hydrogel formulations and the intensity of BP characteristic peak (1725 cm^{-1}) on the surface of hydrogels.

We demonstrated that leaching materials released from phosphate- modified hydrogels were non-toxic, and did not have any effect on hFOB cell viability after 1 and 3 d of culture. The high cell viability observed in this experiment could be associated with the reactivity of unsaturated methacrylate groups in BP and the rapid polymerization rate, resulting in a low amount of unreacted materials. In a previous study, a decreased viability was reported for human marrow stromal cells when exposed to unreacted ethylene glycol methylene phosphate (EGMP) monomer [28]. However, under a photo-crosslinking condition where cell exposure to the raw materials is limited, the monomer was found to be relatively non toxic [28].

hFOB cells seeded on the hydrogel discs exhibited a dramatic change in cell attachment on the surface of phosphate-containing hydrogels. The cells seeded on OPF-BP10, OPF-BP20 and OPF-BP30 had a high proliferation rate and entirely covered the scaffold surfaces over 7 d of culture. hFOB cells exhibited an extended fibroblast-like morphology on these surfaces, suggesting an increased proliferation rate for anchorage-dependent osteoblasts [29]. The results from MTS proliferation assay exhibited at least 5-fold increases in cell number on OPF-BP10, OPF-BP20 and OPF-BP30 surfaces after 7 d in culture. Furthermore, we demonstrated that hFOB cells cultured on OPF-BP20 and OPF-BP30 expressed greater ALP activity. hFOB cells are osteoblast precursor cells which express ALP when they differentiate into a mature osteoblastic phenotype [30]. Increased expression of ALP indicates an increase in osteoblast activity of hFOB cells on phosphate-containing hydrogels.

After incubating the hydrogels in serum-containing media for 1 week, SEM revealed formation of mineral nucleators on the surface of BP-containing scaffolds, while no crystal was observed on the OPF hydrogels without BP. EDAX revealed that the crystals formed on hydrogel surfaces consisted of calcium and phosphorus, and the concentration of calcium immobilized on hydrogel surfaces was a function of phosphorus concentration. However, the Ca/P ratio decreased with increasing phosphate concentration on the surfaces. EDAX analysis of hydroxyapatite showed a Ca/P ratio of1.9 while individual crystals on OPF-BP30 had a Ca/P ratio of 0.23. We also demonstrated the presence of other ions such as Na, Cl, Mg and S within the crystals on phosphate-containing hydrogels. This suggests that negatively charged phosphate groups are capable of attracting positively charged ions from media and altering protein adsorption and integrin–matrix interactions on the surfaces, resulting in increased cell attachment and proliferation.

MSCs also exhibited extended fibroblast-like morphology on BP-modified surfaces similar to those of osteoblasts. Moreover, an increased cell number was observed on the surface of OPF-BP20 and OPF-BP30 hydrogels after 3 and 7 d in culture. We demonstrated that the addition of soluble osteogenic factors increased ALP activity on all surfaces. However, ALP activity was not significantly different on the surfaces except for unmodified hydrogel, which showed a significant increase in ALP activity in osteogenic media as compared to non-osteogenic media. We demonstrated that the MSCs had an increased ALP activity on BP-incorporating scaffolds without the use of osteogenic factors. This finding suggests that phosphate groups tethered to the hydrogel surfaces play a role in differentiation of MSCs into osteoblasts. Dalby and Müller have also reported MSC differentiation into osteoblasts without the use of osteogenic factors [31–33]. In these studies the specific surface topography and chemistry were able to control the structural organization of adsorbed matrix proteins, including collagen I, laminin, fibronectin and integrins, which are necessary

for osteoblast differentiation and mineralization. It has been also shown that osteopontin secreted by seeded human MSCs adsorbs through electrostatic interactions to the calcium phosphate, or hydroxyapatite, enabling the attachment of MSCs to a phosphate-containing polymer [28]. Given these data, it is possible that incorporation of BP into OPF hydrogels provides specific cues on the surface, including the distribution of calcium phosphate ions and protein adsorption, which ultimately influence MSC differentiation.

5. Conclusion

The present study demonstrates the incorporation of a negatively charged phosphate-containing molecule into the OPF hydrogel. We have shown that leaching materials released from phosphate-modified hydrogels were non-toxic, and had no effect on osteoblast viability. Our results revealed that incorporation of phosphate groups improved attachment, proliferation and differentiation of osteoblast precursor cells. Additionally, phosphate-containing hydrogels supported attachment of MSCs that are critical for bone tissue regeneration. Our results revealed that MSCs are able to attach and differentiate into an osteoblastic phenotype without the use of osteogenic factors. These findings suggest that the presence of phosphate on a bone cell attachment surface is an important factor in the subsequent behavior of the cells that anchor on that surface. This could be attributed to the change in surface chemistry and protein absorption on phosphate-containing hydrogel surfaces. Thus, the phosphate-modified OPF hydrogels described in this study represent attractive candidate scaffolds for bone tissue engineering applications.

Acknowledgments

The project described was supported by the Mayo Foundation, NIH Grant R01 EB 03060-6, and Armed Forces Institute of Regenerative Medicine award number W81XWH-08-2-0034. The authors acknowledge the NIH training grant (T32 AR056950) and the Loan Repayment Program from NIH/NIAMs to M.B.R.

References

1. Deshpande AS, Fang PA, Zhang X, Jayaraman T, Sfeir C, Beniash E. Primary structure and phosphorylation of dentin matrix protein 1 (DMP1) and dentin phosphophoryn (DPP) uniquely determine their role in biomineralization. Biomacromolecules. 2011; 12:2933–45. [PubMed: 21736373]
2. Zouani OF, Chollet C, Guillotin B, Durrieu MC. Differentiation of pre-osteoblast cells on poly(ethylene terephthalate) grafted with RGD and/or BMPs mimetic peptides. Biomaterials. 2010; 31:8245–53. [PubMed: 20667411]
3. Zavgorodniy AV, Borrero-Lopez O, Hoffman M, Legeros RZ, Rohanizadeh R. Characterization of the chemically deposited hydroxyapatite coating on a titanium substrate. J Mater Sci Mater Med. 2011; 22:1–9. [PubMed: 21052792]
4. Zhang L, Ayukawa Y, Legeros RZ, Matsuya S, Koyano K, Ishikawa K. Tissue-response to calcium-bonded titanium surface. J Biomed Mater Res A. 2010; 95:33–9. [PubMed: 20740598]
5. Gandhi R, Davey JR, Mahomed NN. Hydroxyapatite coated femoral stems in primary total hip arthroplasty: a meta-analysis. J Arthroplasty. 2009; 24:38–42. [PubMed: 18534435]
6. Marotta JS, Widenhouse CW, Habal MB, Goldberg EP. Silicone gel breast implant failure and frequency of additional surgeries: analysis of 35 studies reporting examination of more than 8000 explants. J Biomed Mater Res. 1999; 48:354–64. [PubMed: 10398041]
7. Rhee SH, Tanaka J. Effect of citric acid on the nucleation of hydroxyapatite in a simulated body fluid. Biomaterials. 1999; 20:2155–60. [PubMed: 10555083]
8. Saiz E, Goldman M, Gomez-Vega JM, Tomsia AP, Marshall GW, Marshall SJ. In vitro behavior of silicate glass coatings on Ti6A14V. Biomaterials. 2002; 23:3749–56. [PubMed: 12109700]

9. Song J, Saiz E, Bertozzi CR. A new approach to mineralization of biocompatible hydrogel scaffolds: an efficient process toward 3-dimensional bonelike composites. J Am Chem Soc. 2003; 125:1236–43. [PubMed: 12553825]
10. Murphy WL, Mooney DJ. Bioinspired growth of crystalline carbonate apatite on biodegradable polymer substrata. J Am Chem Soc. 2002; 124:1910–7. [PubMed: 11866603]
11. Nuttelman CR, Tripodi MC, Anseth KS. Synthetic hydrogel niches that promote hMSC viability. Matrix Biol. 2005; 24:208–18. [PubMed: 15896949]
12. Burdick JA, Ward M, Liang E, Young MJ, Langer R. Stimulation of neurite outgrowth by neurotrophins delivered from degradable hydrogels. Biomaterials. 2006; 27:452–9. [PubMed: 16115674]
13. Shin H, Jo S, Mikos AG. Modulation of marrow stromal osteoblast adhesion on biomimetic oligo[poly(ethylene glycol) fumarate] hydrogels modified with Arg-Gly-Asp peptides and a poly(ethyleneglycol) spacer. J Biomed Mater Res. 2002; 61:169–79. [PubMed: 12061329]
14. Temenoff JS, Shin H, Conway DE, Engel PS, Mikos AG. In vitro cytotoxicity of redox radical initiators for cross-linking of oligo(poly(ethylene glycol) fumarate) macromers. Biomacromolecules. 2003; 4:1605–13. [PubMed: 14606886]
15. Cha MH, Choi J, Choi BG, Park K, Kim IH, Jeong B, et al. Synthesis and characterization of novel thermo-responsive F68 block copolymers with cell-adhesive RGD peptide. J Colloid Interface Sci. 2011; 360:78–85. [PubMed: 21601867]
16. Li L, Wu J, Gao C. Gradient immobilization of a cell adhesion RGD peptide on thermal responsive surface for regulating cell adhesion and detachment. Colloids Surf B: Biointerf. 2011; 85:12–8.
17. You M, Peng G, Li J, Ma P, Wang Z, Shu W, et al. Chondrogenic differentiation of human bone marrow mesenchymal stem cells on polyhydroxyalkanoate (PHA) scaffolds coated with PHA granule binding protein PhaP fused with RGD peptide. Biomaterials. 2011; 32:2305–13. [PubMed: 21190731]
18. Jo S, Shin H, Mikos AG. Modification of oligo(poly(ethylene glycol) fumarate) macromer with a GRGD peptide for the preparation of functionalized polymer networks. Biomacromolecules. 2001; 2:255–61. [PubMed: 11749181]
19. Dadsetan M, Knight AM, Lu L, Windebank AJ, Yaszemski MJ. Stimulation of neurite outgrowth using positively charged hydrogels. Biomaterials. 2009; 30:3874–81. [PubMed: 19427689]
20. Dadsetan M, Pumberger M, Casper ME, Shogren K, Giuliani M, Ruesink T, et al. The effects of fixed electrical charge on chondrocyte behavior. Acta Biomater. 2011; 7:2080–90. [PubMed: 21262395]
21. Sosnik A, Sefton MV. Poloxamine hydrogels with a quaternary ammonium modification to improve cell attachment. J Biomed Mater Res A. 2005; 75:295–307. [PubMed: 16059894]
22. Dadsetan M, Szatkowski JP, Yaszemski MJ, Lu L. Characterization of photo-cross-linked oligo[poly(ethylene glycol) fumarate] hydrogels for cartilage tissue engineering. Biomacromolecules. 2007; 8:1702–9. [PubMed: 17419584]
23. Dadsetan M, Liu Z, Pumberger M, Giraldo CV, Ruesink T, Lu L, et al. A stimuli-responsive hydrogel for doxorubicin delivery. Biomaterials. 2010; 31:8051–62. [PubMed: 20696470]
24. Harris SA, Enger RJ, Riggs BL, Spelsberg TC. Development and characterization of a conditionally immortalized human fetal osteoblastic cell line. J Bone Miner Res. 1995; 10:178–86. [PubMed: 7754797]
25. Sarikaya M. Biomimetics: materials fabrication through biology. Proc Natl Acad Sci USA. 1999; 96:14183–5. [PubMed: 10588672]
26. Wang S, Kempen DH, Yaszemski MJ, Lu L. The roles of matrix polymer crystallinity and hydroxyapatite nanoparticles in modulating material properties of photo-crosslinked composites and bone marrow stromal cell responses. Biomaterials. 2009; 30:3359–70. [PubMed: 19339048]
27. Wang S, Lu L, Gruetzmacher JA, Currier BL, Yaszemski MJ. Synthesis and characterizations of biodegradable and crosslinkable poly(epsilon-caprolactone fumarate), poly(ethylene glycol fumarate), and their amphiphilic copolymer. Biomaterials. 2006; 27:832–41. [PubMed: 16102819]
28. Nuttelman CR, Benoit DS, Tripodi MC, Anseth KS. The effect of ethylene glycol methacrylate phosphate in PEG hydrogels on mineralization and viability of encapsulated hMSCs. Biomaterials. 2006; 27:1377–86. [PubMed: 16139351]

29. Baxter LC, Frauchiger V, Textor M, Gwynnap I, Richards RG. Fibroblast and osteoblast adhesion and morphology on calcium phosphate surfaces. Eur Cell Mater. 2002; 4:1–17. [PubMed: 14562250]

30. Hicok KC, Thomas T, Gori F, Rickard DJ, Spelsberg TC, Riggs BL. Development and characterization of conditionally immortalized osteoblast precursor cell lines from human bone marrow stroma. J Bone Miner Res. 1998; 13:205–17. [PubMed: 9495513]

31. McMurray RJ, Gadegaard N, Tsimbouri PM, Burgess KV, McNamara LE, Tare R, et al. Nanoscale surfaces for the long-term maintenance of mesenchymal stem cell phenotype and multipotency. Nat Mater. 2011; 10:637–44. [PubMed: 21765399]

32. Dalby MJ, Gadegaard N, Tare R, Andar A, Riehle MO, Herzyk P, et al. The control of human mesenchymal cell differentiation using nanoscale symmetry and disorder. Nat Mater. 2007; 6:997–1003. [PubMed: 17891143]

33. Muller P, Bulnheim U, Diener A, Luthen F, Teller M, Klinkenberg ED, et al. Calcium phosphate surfaces promote osteogenic differentiation of mesenchymal stem cells. J Cell Mol Med. 2008; 12:281–91. [PubMed: 18366455]

Appendix A. Figures with essential color discrimination

Certain figures in this article, particularly Figures 6, 8 and 9, are difficult to interpret in black and white. The full color images can be found in the on-line version, at doi:10.1016/j.actbio.2011.12.031.

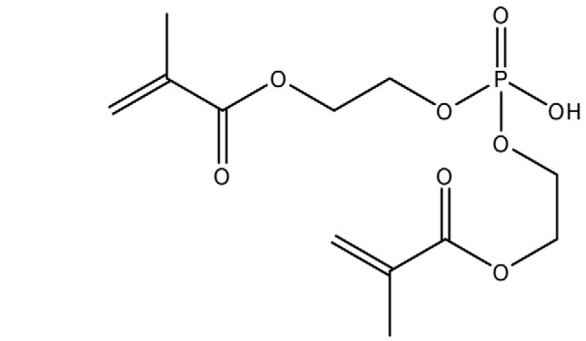

Bis(2-(methacryloyloxy)ethyl) phosphate (BP)

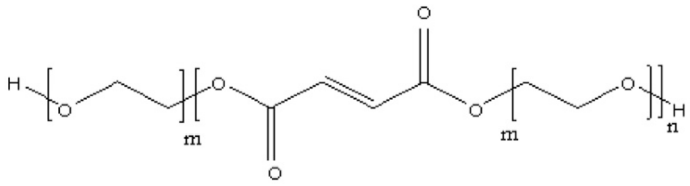

Oligo (poly(ethylene glycol) fumarate) (OPF)

Fig. 1.
Chemical structures of oligo(polyethylene glycol) fumarate (OPF), and bis(2-methacryloyloxy)ethyl) phosphate (BP).

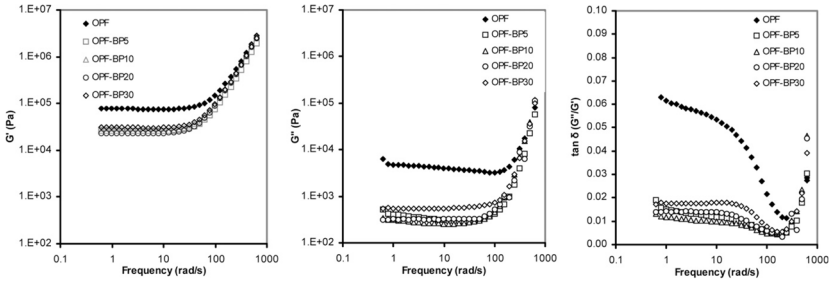

Fig. 2.

Storage modulus G′ (left panel), loss modulus G″ (middle panel) and viscosity η (right panel) vs. frequency of unmodified hydrogel (OPF) compared to hydrogels with varying concentrations of BP (OPF-BP).

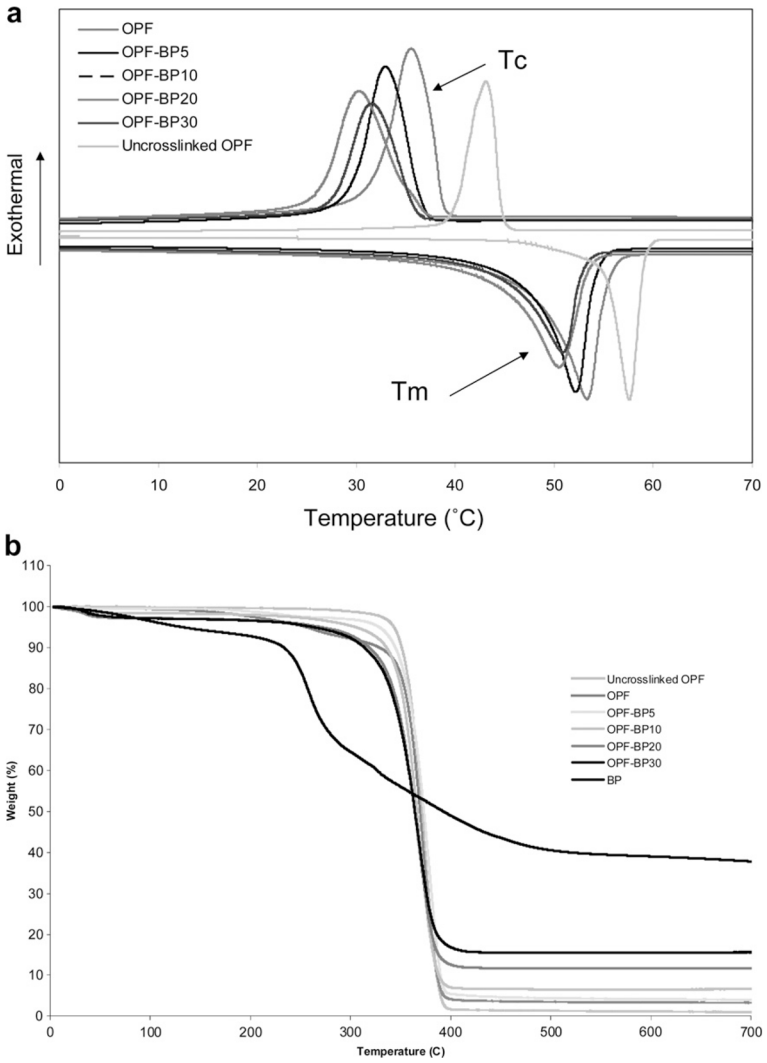

Fig. 3.

(a) DSC curves for OPF and BP-modified hydrogels. Three consecutive heat/cool/heat cycles were used to determine melting points (Tm), crystallization temperature (Tc) and heats of fusion (ΔTm). (b) TGA curves used to determine onset of degradation (Td) for OPF and BP-modified hydrogels.

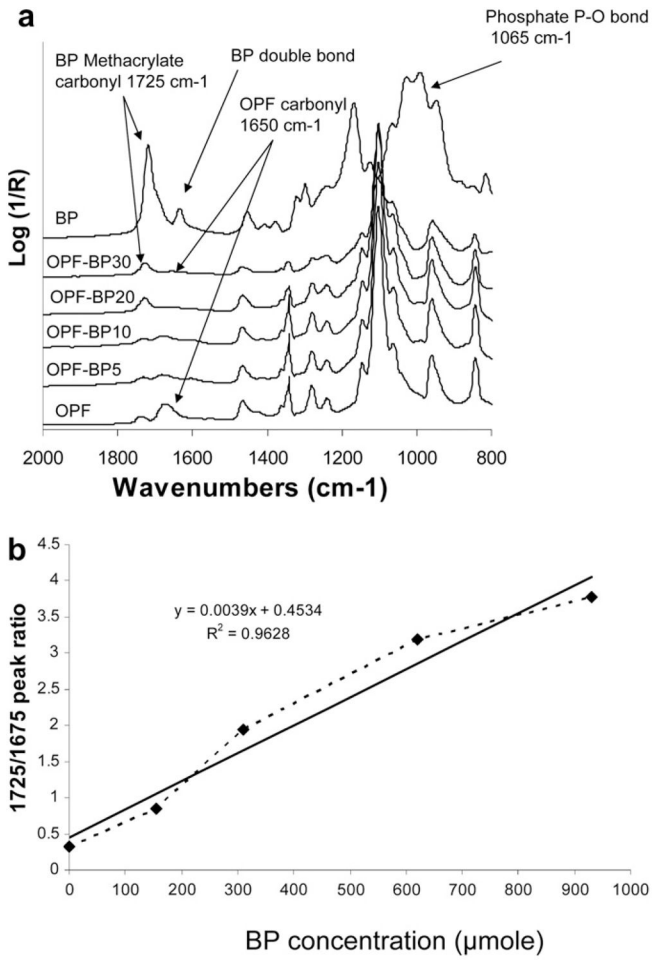

Fig. 4.

(a) Micro-ATR-FTIR of unmodified BP-modified hydrogels after crosslinking and lyophilization. With increasing BP concentration in hydrogel formulations, the peak intensity at 1725 cm^{-1} assigned to methacrylate groups from BP increased, and the peak intensity at 1650 cm^{-1} assigned to carbonyl from OPF decreased. (b) The linear relationship between the amounts of BP added to the OPF solution and the levels of covalently coupled BP in crosslinked hydrogels. The solid line is a linear fit of the data (R^2 = 0.9628).

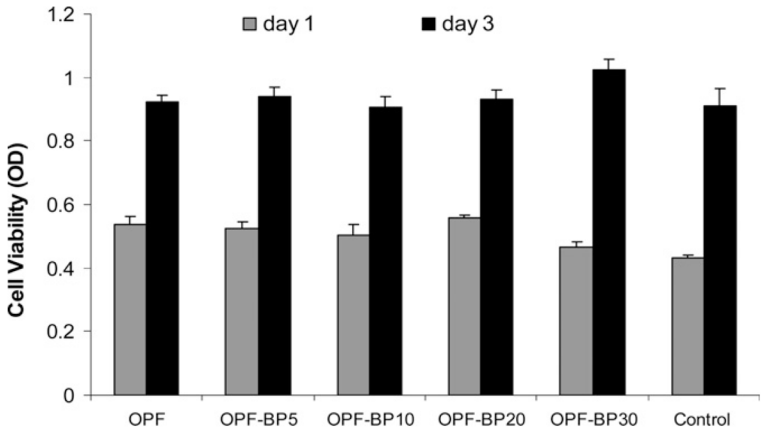

Fig. 5.

Toxicity of leaching materials from hydrogels after 1 and 3 d in culture. hFOB cells were plated on 24-well tissue culture plates and exposed to leaching materials from scaffolds via transwell inserts. The viability of the cells was tested using the MTS Cell Proliferation Assay by measuring the optical density (OD) at 490 nm. Values represent mean ± standard error (n = 3).

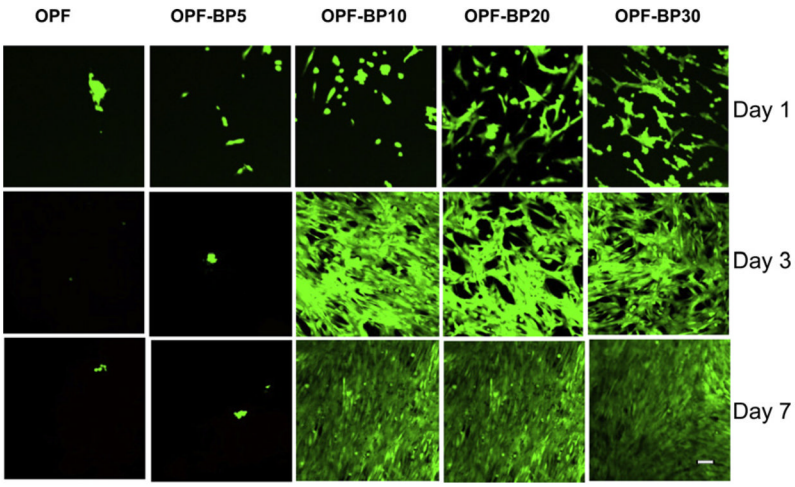

Fig. 6.

Osteoblast viability on hydrogels with different concentrations of BP in their formulation on days 1, 3 and 7. Viable cells are stained green and dead cells are stained red. Scale bar = 20 μm.

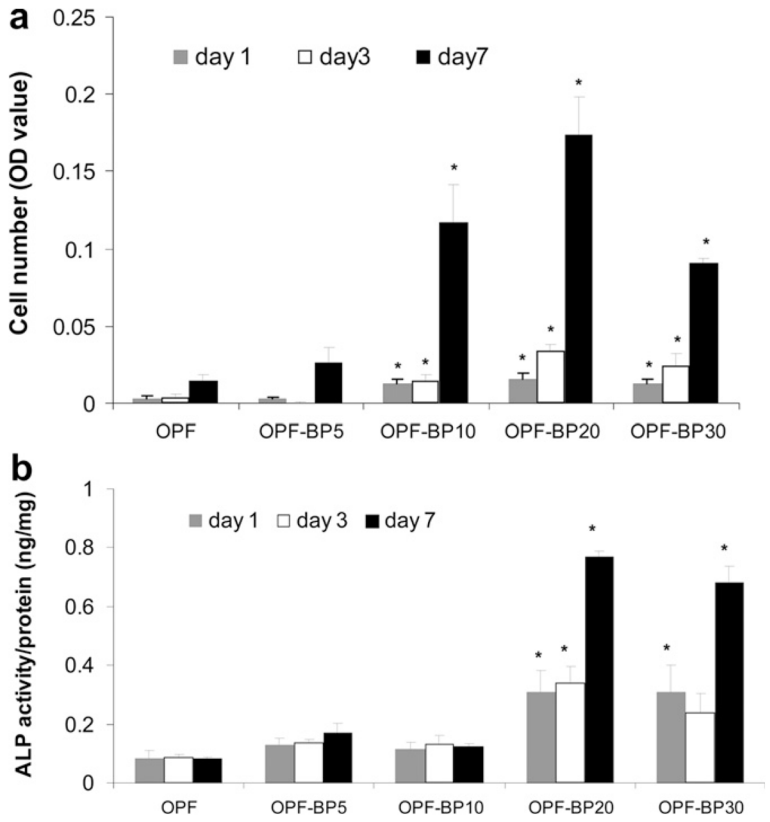

Fig. 7.

(a) Proliferation of hFOB cells on OPF hydrogels with varying amounts of BP at days 1, 3 and 7. Cell number was determined using the MTS Cell Proliferation Assay by measuring the optical density (OD) at 490 nm. (b) ALP activity of hFOB cells on OPF hydrogels with varying concentrations of BP in their formulation on days 1, 3 and 7. Values represent mean ± standard error ($n = 3$). $^{*}P < 0.005$ significantly different as compared to unmodified OPF hydrogel.

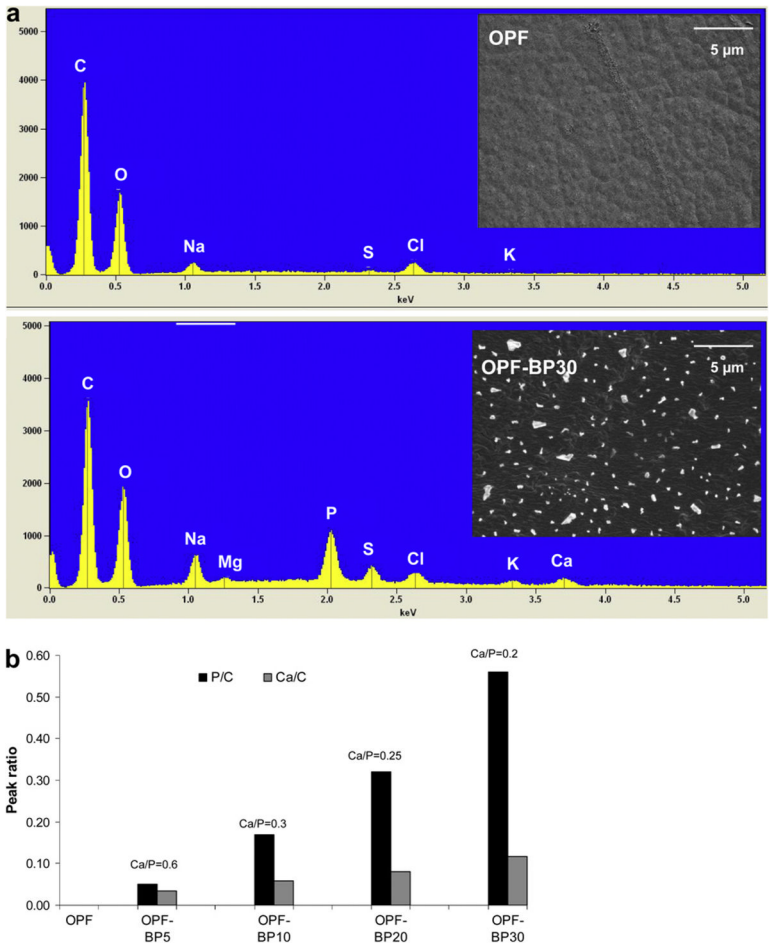

Fig. 8.

(a) SEM images and EDAX spectra of OPF (unmodified) and OPF-BP30 (hydrogel with 930 μmol BP). (b) Comparison of calcium and phosphorus peaks on the hydrogel surfaces as a function of BP concentration. The peak heights of both calcium and phosphorous are normalized to the carbon peak height. The Ca/P ratio was obtained from area analysis.

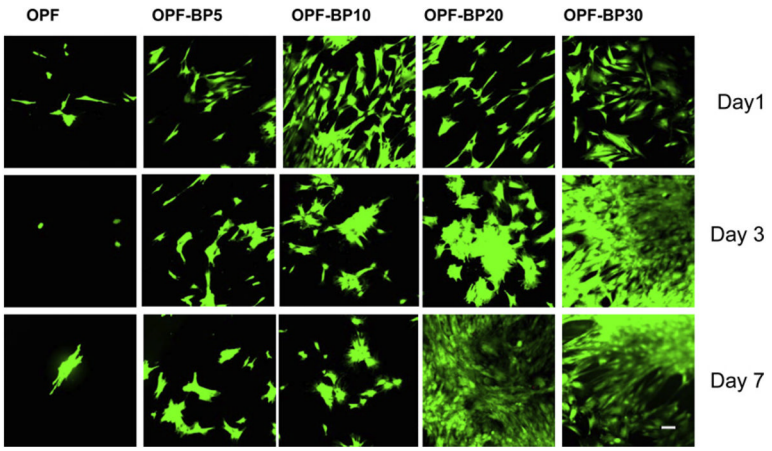

Fig. 9.

MSC viability on hydrogels with different concentrations of BP in their formulation on days 1, 3 and 7. Viable cells are stained green and dead cells are stained red. Scale bar = 20 μm.

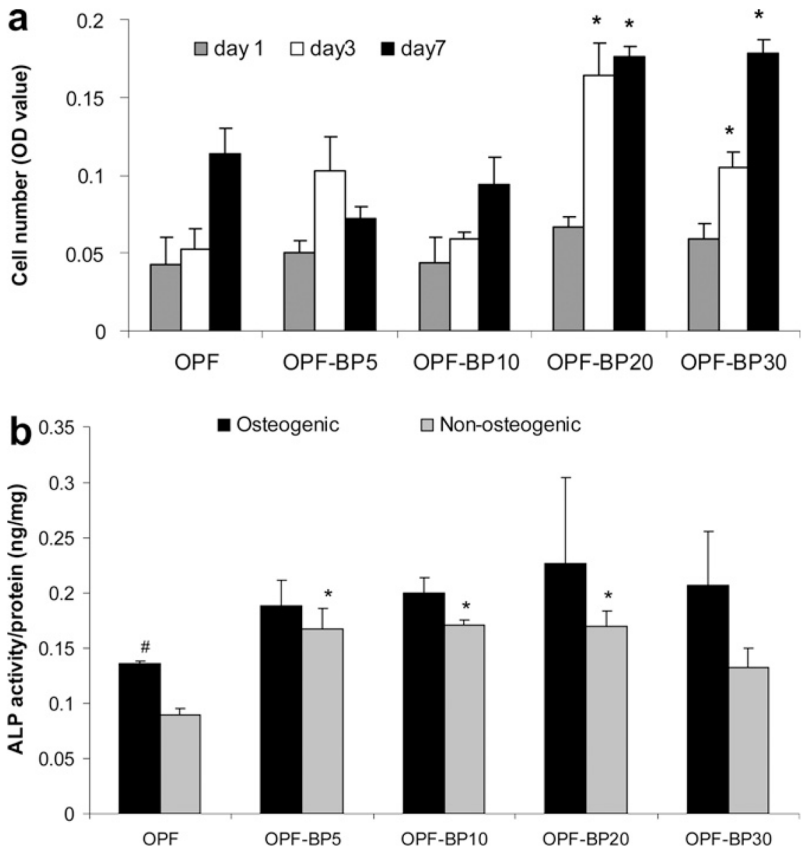

Fig. 10.

(a) Proliferation of MSCs on OPF hydrogels with varying concentrations of BP in their formulation on days 1, 3 and 7. Cell number was determined using the MTS Cell Proliferation Assay by measuring the optical density (OD) at 490 nm. $^{*}P < 0.05$ significantly different as compared to unmodified OPF hydrogel at the same time point. (b) ALP activity of MSCs on OPF hydrogels with different concentrations of BP in osteogenic and non-ostegenic media after 7 days in culture. $^{*}P < 0.05$ significantly different as compared to unmodified OPF hydrogel in the same media, $\#P < 0.05$ significantly higher in osteogenic media. Values represent mean ± standard error ($n = 3$).

Table 1

Characterization of hydrogels with different BP concentrations.

Hydrogel formulations	BP concentration (μmol)	Swelling ratio	Sol fraction (%)	Compressive modulus (MPa)
OPF	0	5.47 ± 0.09	7.01 ± 0.12	0.028 ± 0.003
OPF-BP5	155	6.09 ± 0.10[a]	7.07 ± 0.40	0.029 ± 0.005
OPF-BP10	310	6.13 ± 0.04[a]	7.16 ± 0.38	0.037 ± 0.002[a]
OPF-BP20	620	6.12 ± 0.05[a]	7.06 ± 0.25	0.030 ± 0.009
OPF-BP30	930	6.96 ± 0.31[ab]	8.08 ± 0.80[a]	0.020 ± 0.001[a]

[a] Significantly different from unmodified OPF hydrogel ($P < 0.05$).

[b] Significantly different from all other hydrogels ($P < 0.05$).

Table 2

Hydrogel thermal properties.

Hydrogel formulations	Tm (°C)	ΔHm (J/g)	Tc (°C)	ΔHc (J/g)	%c[a]	Td (°C)
Uncrosslinked OPF	57.8	130.9	41.9	116.8	63.5	335
OPF	53.3	88.9	38.8	94.5	43.2	334
OPF-BP5	52.7	83.1	33.0	89.0	40.4	331
OPF-BP10	51.5	80.4	31.9	87.3	39.1	326
OPF-BP20	50.5	71.4	30.3	74.5	34.7	317
OPF-BP30	50.9	60.0	31.6	58.6	29.1	315

[a]Calculated using the ΔHm of PEG, 205.81(J/g) (Ref. [27]).